PCCP

Accepted Manuscript

This is an *Accepted Manuscript*, which has been through the Royal Society of Chemistry peer review process and has been accepted for publication.

Accepted Manuscripts are published online shortly after acceptance, before technical editing, formatting and proof reading. Using this free service, authors can make their results available to the community, in citable form, before we publish the edited article. We will replace this *Accepted Manuscript* with the edited and formatted *Advance Article* as soon as it is available.

You can find more information about *Accepted Manuscripts* in the Information for Authors.

Please note that technical editing may introduce minor changes to the text and/or graphics, which may alter content. The journal's standard Terms & Conditions and the Ethical guidelines still apply. In no event shall the Royal Society of Chemistry be held responsible for any errors or omissions in this *Accepted Manuscript* or any consequences arising from the use of any information it contains.

ROYAL SOCIETY OF CHEMISTRY

www.rsc.org/pccp

Graphical abstract

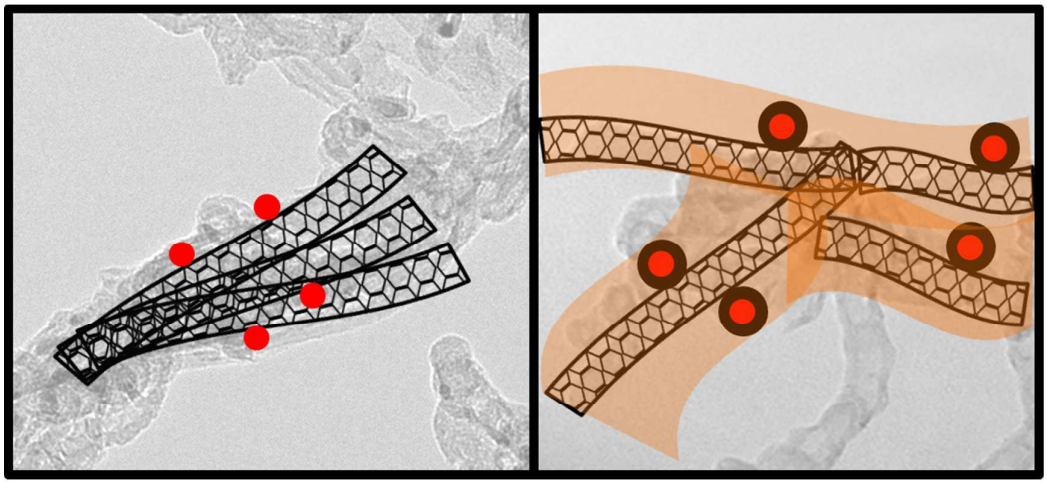

A new kind of biocomposite, as-prepared carbon nanotubes-chitosan (APCNTs-CS), was prepared and characterized.

Physical Chemistry Chemical Physics Accepted Manuscript

A Facile Method for Synthesis of Magnetic CNTs/C@Fe/Chitosan Composite and their Applications for Tetracycline Removal from Aqueous Solutions

Jie Ma[a]*, Yuan Zhuang[a], Fei Yu[a,b]*

[a] State Key Laboratory of Pollution Control and Resource Reuse, School of Environmental Science and Engineering, Tongji University, 1239 Siping Road, Shanghai 200092, P. R. of China.

[b] College of chemistry and environmental engineering, Shanghai Institute of Technology, Shanghai 2001418, China.

*Corresponding author.

Jie Ma: Tel.: +86 21 65981831; Fax: +86 21 65981831. E-mail: jma@tongji.edu.cn;

Fei Yu: Tel: +86 21 60873182;Fax: +86 21 60873182. Email: fyu@vip.163.com;

Physical Chemistry Chemical Physics Accepted Manuscript

Abstract:

Magnetic CNTs/C@Fe/chitosan composite(CNTs/C@Fe/CS) was prepared based on the as-prepared carbon nanotubes(APCNTs), metal nanoparticles in APCNTs can be utilized directly without any purification treatment, and the carbon shells provide an effective barrier against oxidation, acid dissolution, and movement of MNPs, and thus ensure a long-term stability of CNTs/C@Fe/CS. The results showed that CNTs/C@Fe/CS contained more abundant oxygen and nitrogen containing functional groups after chitosan modification and the composite had good magnetization characteristics, even in acid solutions. And then CNTs/C@Fe/CS was used as an adsorbent for removal of tetracycline from aqueous solutions. Adsorption experiments indicated that CNTs/C@Fe/CS have good adsorption capacity (q_e) of tetracycline (104 mg/g). The Freundlich isotherm model fitted the experiment data better than the Langmuir isotherm mode. Kinetic regression results showed that the adsorption kinetics was more accurately represented by a pseudo second-order model. Intra-particle diffusion was involved in the adsorption, but it was not the only rate-controlling step. Cu^{2+} and humic acid could promote the adsorption of tetracycline on CNTs/C@Fe/CS. The CNTs/C@Fe/CS adsorbents could be effectively and quickly separated by applying an external magnetic field and the adsorption capacity still maintained 99.3 mg/g at after 10 times. Therefore, CNTs/C@Fe/CS is a promising magnetic nanomaterial for preconcentration and separation of organic pollutants for environmental remediation.

Keywords: Carbon nanotube; Chitosan; Adsorption; Tetracycline; Magnetic separation;

Physical Chemistry Chemical Physics Accepted Manuscript

1. Introduction

Antibiotics are of concern due to their potential genotoxic effects, disruption of aquatic ecosystems, promotion of antibiotic resistance, complications for water reuse, and even increased human health risks[1]. Hence, the issue of antibiotics and their removal from water resources is an urgent research subject[2]. Antibiotics are widely used around the world in medical care and the farming industry. However, they have received increasing attention in recent years because they are toxic to living beings. Exposures to residues of antibiotics and their transformed products might cause a variety of adverse effects, including acute and chronic toxicity, and microorganism antibiotic resistance[3]. Hence, there is an increasing demand for the removal of antibiotics from water. Many kinds of antibiotics can be degraded in soils and water, which will reduce their potency; however, some degradation products may have similar toxicity to their parent compound[4]. Additional treatment steps, downstream of conventional biological process, such as membrane processes[5], adsorptive treatment processes[6, 7], advanced oxidation processes[8], and the combined ones[9], have been suggested and investigated to eliminate micropollutants. Thus, adsorption is an effective method to remove antibiotics. Tetracyclines are broad-spectrum agents, exhibiting activity against a wide range of gram-positive and gram-negative bacteria, atypical organisms such as chlamydiae, mycoplasmas, and rickettsiae, and protozoan parasites [10]. Though a comparative study, Ji *et al.* [11] found that microporous activated carbons exhibited much lower adsorption affinity for bulky tetracycline molecules mainly due to the molecular sieving effect. Moreover, as a special adsorbent for organic contaminants, carbon nanotubes can be engineered and functionalized on purpose to enhance the adsorption selectivity specific to the target compound. The results of the present work indicate that the adsorption selectivity and efficiency can be improved through specific molecular-level interactions between organic contaminants and carbon nanotubes. Thus, carbon nanomaterial has great potential for applications in antibiotics adsorption.

Physical Chemistry Chemical Physics Accepted Manuscript

Carbon nanotubes (CNTs), which are considered to be extremely superior sorbents due to their high specific surface area and large microspore volume, have been utilized for the sorption of a number of different organic compounds[12, 13]. However, there is potential for CNTs to become another source of environmental contaminant if the use of CNTs is not responsibly managed. Compared with traditional centrifugation and filtration methods, the magnetic separation method is considered as a rapid and effective technique for separating adsorbents from environmental applications[14].

Chemical oxidation polymerization, followed by the carbonization process has been employed to produce iron oxide-impregnated magnetic CNT composites. A solvo-thermal method has been also used to synthesize CNT–iron oxide composites. Other effective approaches, including the arc-discharge technique and electrolysis deposition, to prepare CNT-based functional materials have been developed [15]. However, traditional synthesis methods of magnetic CNTs are complex and environmentally unfriend[16]: a) as prepared carbon nanotubes (APCNTs) usually were firstly purified using strong acid to remove metal particles and carbonaceous by-products, purified CNTs need to be modified with functional groups using oxidation agents, and then iron oxide nanoparticles can be loaded successfully on the wall or interior space of purified CNTs. Besides, uncovered magnetic nanoparticles may agglomerate when a magnetic field is applied, and bare nanoparticles could be oxidized in air or erode under acidic conditions. As a result, the synthesis process is expensive and time-consuming with a low yield. These issues may ultimately hinder widespread practical applications of the magnetic CNTs composite.

Chitosan (CS) is a biopolymer that has been widely used as a material to which tissue cells are attached, biomolecules are entrapped, or enzymes are immobilized [17]. Incorporation of super strong lightweight carbon nanotube structures into CS matrix offers a novel approach to the design of high performance composite materials with better properties. However, the atomically smooth graphene surface of nanotubes can provide only limited load transfer from the matrix to nanotubes across the nanotube/polymer interface because of weak Van der Waals interfacial bonding

Physical Chemistry Chemical Physics Accepted Manuscript

through covalent grafting of carbon nanotubes to the CS to form nanocomposites. Commonly, chitosan and carbon nanotubes were covalently grafted to composites using ultrasonic assisted acid oxidation of nanotubes followed by thionylation and dispersion in CS [18]. To obtain CNTs with more functional groups and lower toxicity, chitosan is usually used to modify CNTs. Qian *et al.* [19] prepared a composite film of carbon nanotubes and chitosan for application as amperometric hydrogen peroxide biosensor. Carson *et al.* [18] reported chitosan–carbon nanotube composites for bone tissue engineering. Chen *et al.* [20] prepared chitosan/multi-walled carbon nanotubes/hydroxyapatite nano-composite for bone tissue engineering.

In this paper, we report a facile method to synthesize magnetic CNTs/C@Fe/CS using APCNTs modified by CS. This facile synthesis method has the following advantages: a) metal nanoparticles in APCNTs can be utilized directly without any purification treatment; b) the carbon shells provide an effective barrier against oxidation, acid dissolution, and movement of nanoparticles, and thus ensure a long-term stability of nanoparticles[21]. c) chemical functionalization decreases the toxicity and increase the hydrophily[22, 23]. And then, CNTs/C@Fe/CS was used as adsorbents to remove tetracycline from aqueous solutions, which exhibited excellent adsorption. The adsorption capacities are higher than what have been shown in previous reports[24-27]. After adsorption, the CNTs/C@Fe/CS adsorbents could be effectively and immediately separated using a magnet, thereby reducing the potential risks from nanoparticles as an environmental contaminant. Therefore, CNTs/C@Fe/CS may be a promising magnetic adsorbent for removing pollutants.

2. Experimental

2.1Materials and chemicals

All chemicals were purchased from Sinopharm Chemical Reagent Co., Ltd (Shanghai, China) in analytical purity and used in the experiments directly without any further purification. All solutions were prepared using deionized water.

Physical Chemistry Chemical Physics Accepted Manuscript

The CNTs/C@Fe were prepared using a CVD method [28]. Ethanol was used as the carbon feedstock; ferrocene was used as the catalyst; and thiophene was used as the growth promoter. Argon flow was introduced in the quartz tube in order to eliminate oxygen from the reaction chamber. The ethanol solution dissolved with ferrocene and thiophene was supplied by an electronic squirming pump and sprayed through a nozzle with an argon flow. After several hours of pyrolysis, the supply of ethanol was terminated, and the CNTs/C@Fe were collected from a collecting unit connected to the quartz tube. 1g of CS and 1g of carbon nanotubes were mixed in 100 mL 5 wt % dilute acetic acid solution and stirred for 5-10 min; then 0.6 g $NaHSO_3$ was added and stirred till the bubbles became uniformly, and added formaldehyde solution, the solution was stirred for 5 min to become uniform and then stood 10 min. The mixture was filtered and washed by distilled water, and then it was put into NaOH solution under pH 10. 10ml epichlorohydrin was added into the above-mentioned mixture. The mixture was heated under 90℃ for 6h followed by filtering and washing by distilled water.

2.2 Batch adsorption experiments

Batch experiments were conducted to evaluate the adsorption performance of tetracycline on the CNTs/C@Fe/CS. 100 mg/L stock tetracycline solution was prepared by dissolving 100mg tetracycline in 1L deionized water. Working solutions of the required concentrations were obtained by diluting the stock solution with deionized water. All the sorption tests were conducted in well-capped 100 mL flasks containing 20 mL tetracycline solution with required concentration. After 10 mg of adsorbent was added, the flasks were shaken in a thermostatic shaker at 150 rpm at 298K for 24 h. All the adsorption experiments were conducted in duplicate, and only the mean values were reported. The maximum deviation for the duplicates was usually less than 5%. The blank experiments without the addition of adsorbent were conducted to ensure that the decrease in the concentration was actually due to the adsorption rather than by the adsorption on the glass bottle wall. After adsorption, the adsorbent was separated by a 0.45 μm membrane. The residual concentrations in

Physical Chemistry Chemical Physics Accepted Manuscript

solution were determined by an ultraviolet spectrophotometer (Tianmei UV-2310(II)) through measuring absorbance changes at 364 nm. The adsorption isotherm was studied at pH 6 and the initial concentration solution was set from 1 mg/L to 50 mg/L. The adsorption capacity (mg/g) was calculated as equation (1).

$$q_t = (C_0 - C_t) \times \frac{V}{m} \qquad (1)$$

where C_0 and C_t are the initial concentrations and concentrations after a period of time (mg/L); V is the initial solution volume (L); and m is the adsorbent dosage(g).

The adsorption isotherm was calculated by Langmuir, Freundlich, Temkin and Dubinin-Radushkevich (D-R) isotherms as in equations (2) to (6). The Langmuir isotherm assumes that the adsorbate forms a monolayer around the homogenous surface of the adsorbent and that there is no interaction between the adsorbed molecules. The Freundlich model is an empirical one, which assumes that adsorption takes place on a heterogeneous surface and also proposes multilayer sorption with interaction among the adsorbed molecules.

The Temkin model is a proper model for the chemical adsorption based on strong electrostatic interaction between positive and negative charges. The D-R isotherm model does not assume a homogenous surface. Furthermore, the effect of the isotherm shape was studied to understand whether an adsorption system is favorable or not. Another important parameter, R_L, called the separation factor or equilibrium parameter, which can be used to determine the feasibility of adsorption in a given concentration range over adsorbent, was also evaluated by equation (7). The mean free energy of adsorption E_{DR} is related through equation (8) [29].

$$\frac{C_e}{q_e} = \frac{1}{K_L} + (\frac{\alpha_L}{K_L})C_e \qquad (2)$$

$$Inq_e = InK_F + \frac{1}{\mathrm{n}} \mathrm{In}C_e \qquad (3)$$

$$q_e = B_T InC_e + B_T \mathrm{In}K_F \qquad (4)$$

$$Inq_e = Inq_m - \beta\varepsilon^2 \qquad (5)$$

$$\varepsilon_e = RTIn(1 + \frac{1}{C_e}) \qquad (6)$$

Physical Chemistry Chemical Physics Accepted Manuscript

$$R_L = \frac{1}{1 + K_L C_0} \quad (7)$$

$$E_{DR} = \frac{1}{(2\beta)^{0.5}} \quad (8)$$

where K_L(L/g) and a_L(L/mg) are the Langmuir isotherm constants, respectively, and a_L relates to the energy of adsorption. When C_e/q_e is plotted against C_e, a straight line will be obtained. The value of K_L can be obtained from the intercept, which is $1/K_L$, and the value of a_L can be obtained from the slope, which is a_L/K_L. The maximum adsorption capacity of the adsorbent, $q_{m,cal}$, i.e., the equilibrium monolayer capacity or saturation capacity, is numerically equal to K_L/a_L; K_F, B_T, K_T are adsorption constants of Freundlich and Temkin models, respectively, and n is the Freundlich linearity index. The Langmuir model is an ideal model that has a perfect adsorbent surface and monolayer molecule adsorption. As an empirical model, the Freundlich model is used widely in the field of chemistry. R (8.314 J/mol K) is the ideal gas constant and T (K) is the absolute temperature.

For a kinetic adsorption study, three common kinetic models (pseudo-first-order (9) that is based on solid capacity, pseudo-second-order (10) that is based on solid phase adsorption and intra-particle diffusion model (11) that describes the diffusion mechanism) were used to fit the experimental data and the correlation coefficient (R^2) was considered as a measurement of the agreement between the experimental data and the two proposed models [30].

$$\ln(q_e - q_t) = \ln q_e - \frac{k_1}{2.303} t \quad (9)$$

$$\frac{t}{q_t} = \frac{1}{k_2 q_e^2} + \frac{t}{q_e} \quad (10)$$

$$q_t = k_{id} t^{0.5} + C \quad (11)$$

where q_e and q_t are the amounts of tetracycline adsorbed (mg/g) at equilibrium and time t (h), respectively; k_1 is the rate constant of the pseudo first-order kinetic model (t^{-1}); k_2 is the rate constant (g/mg·h) of the pseudo second-order kinetic model for adsorption; k_{id} (mg/g·$h^{0.5}$) is the intra-particle diffusion rate constant, C (mg/g) is the adsorption capacity calculated from this model.

Physical Chemistry Chemical Physics Accepted Manuscript

For desorption study, the CNTs/C@Fe/CS after adsorption was magnetically collected, washed with deionized water, and stirred for 24 h in 20 mL of 1 mol/L $NaHSO_3$.The adsorption/desorption cycle was repeated ten times.

2.3 Characterization methods

The microstructure and morphology of CNTs/C@Fe were analyzed using high resolution transmission electron microscopy (HRTEM, JEOL 2100F, accelerating voltage of 200 kV, Japan). The X-ray diffractometer (Bruker D8 Advance, Germany) was operated at 40 kV and 40 mA. A TA Instrumentss Q600 SDT thermal analyser was used for high resolution thermogravimetric analysis (TGA) and differential thermal analysis (DTA) of CNTs/C@Fe and CNTs/C@Fe/CS. The magnetization was measured using a superconducting quantum interference device magnetometer (MPMS XL7, Quantum Design). X-Ray photoelectron spectroscopic (XPS) analysis was carried out in a Kratos Axis Ultra DLD spectrometer, using monochromated Al Ka X-rays.

3. Results and discussion

3.1 Characterization of CNTs/C@Fe/CS

3.1.1 Morphology and structure of CNTs/C@Fe/CS

Fig. 1 shows the transmission electron microscopy (TEM) images of CNTs/C@Fe (Fig. 1a and 1b) and CNTs/C@Fe/CS (Fig. 1c and 1d), it can be seen that the nanotubes were decorated with iron nanoparticles covered by carbon layers. Moreover, CNTs/C@Fe has a fibrous morphology and the diameter is below 50 nm, as shown in Fig. 1b. In CNTs/C@Fe/CS, as shown in Fig. 1d, the tubes are connected to each other in parallel by CS and the agglomeration degrees are obviously lower than CNTs/C@Fe. It can be inferred that the tubes are cross-linked by CS. To further investigation of structure, the X-ray diffraction (XRD) patterns of CNTs/C@Fe and CNTs/C@Fe/CS are tested as shown in Fig. 2. It can be seen that the CNTs/C@Fe were a mixture of two phases: Fe and CNTs. In CNTs/C@Fe/CS, the carbon nanotubes and the Fe still has strong peaks indicating they maintained their structures after CS modification, and the Fe nanoparticles have not been oxidized.

Physical Chemistry Chemical Physics Accepted Manuscript

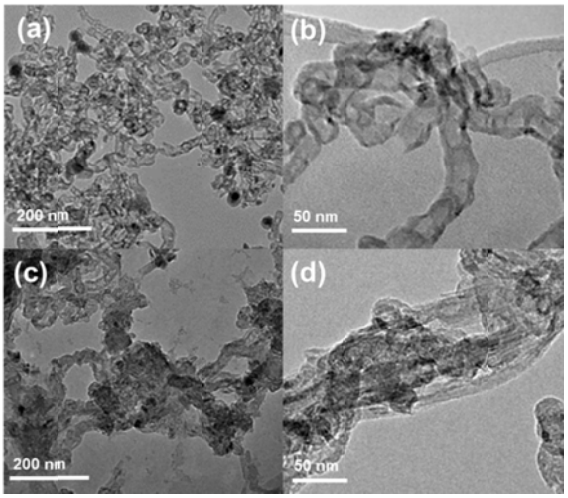

Fig.1 TEM of CNTs/C@Fe (a) and (b), CNTs/C@Fe/CS (c) and (d).

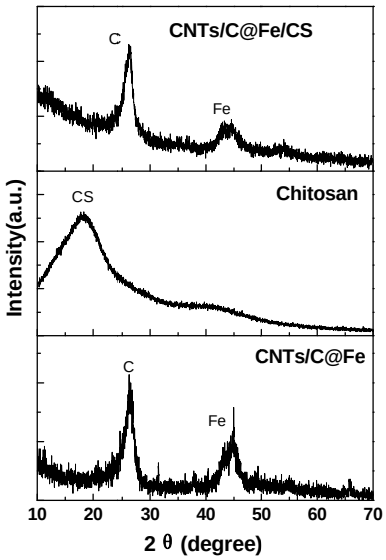

Fig. 2 XRD of CNTs/C@Fe, CS and CNTs/C@Fe/CS.

3.1.2 Composition of CNTs/C@Fe/CS

X-ray photoelectron spectroscopy (XPS) was employed to analyze the surface chemical composition, as shown in Fig. 3. After functionalization, the new peaks of S and N appeared. For the C 1s spectra as shown in Fig. 3b, the strongest peak at 284.6 eV is assigned to C-C for CNTs and results from non-functionalized carbon and the peak at the binding energy of about 285.1 eV is a consequence of single-bonding carbon for CNTs. In O1s spectra as shown in Fig. 2c, peak at 531.5 eV is assigned to C=O. In N1s spectra in Fig. 2d,

Physical Chemistry Chemical Physics Accepted Manuscript

peak at 400.2 eV is assigned to -NH- groups. The O1s in CNTs/C@Fe/CS is stronger than in CNTs/C@Fe and the N1s appears in CNTs/C@Fe/CS rather than in CNTs/C@Fe, indicating that CS has good combination with CNTs/C@Fe and brings abundant oxygen and nitrogen containing functional groups into the composite.

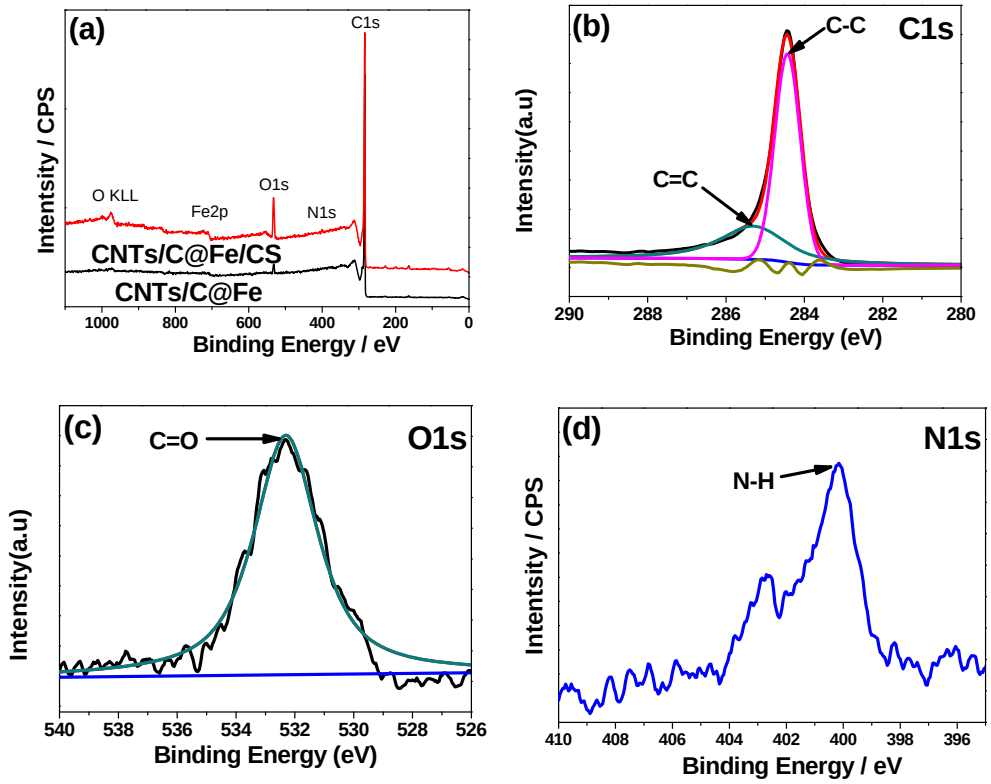

Fig. 3 XPS survey scans(a) of the CNTs/C@Fe/CS and CNTs/C@Fe, the core peaks of C 1s (b), O 1s (c), and N1s (d).

The thermogravimetric analysis (TGA) results of CNTs/C@Fe and CNTs/C@Fe/CS are presented in Fig. 4a. The final weight of the remaining samples is 14% (CNTs/C@Fe) and 13% (CNTs/C@Fe/CS) of the original weight. Assuming that the final material is Fe_2O_3, the quantity of Fe in the CNTs/C@Fe (4.9 %) is lower than that in the CNTs/C@Fe/CS (4.6 %). The reduction in the weight fraction of iron in CNTs/C@Fe/CS can be attributed to the addition of GS. The main thermal events may be identified from DTA curves. Comparing CNTs/C@Fe with CNTs/C@Fe/CS, it is clearly seen that

Physical Chemistry Chemical Physics Accepted Manuscript

the main thermal events temperature (T_m) decreased from ~570 to ~500 °C, which may be attributed to the CNTs/C@Fe/CS structure defects and more oxygen-containing functional groups [16] brought from CS. The thermal event temperature is so high that CNTs/C@Fe/CS could readily meet the application needs of adsorbents in water treatment [21].

3.1.3 Magnetic properties of CNTs/C@Fe/CS

The magnetization characteristics of CNTs/C@Fe and CNTs/C@Fe/CS was investigated at room temperature (Fig. 4b). The saturation magnetization *Ms* of CNTs/C@Fe is 9 emu/g and CNTs/C@Fe/CS is 8 emu/g, which indicated that CNTs/C@Fe/CS still has good magnetization property. The loop of CNTs/C@Fe/CS exhibits very low coercive field (16 Oe) and remanence values (2 emu/g), which can be beneficial for the reuse without reunite for magnetization. It can be found from the insets of Fig. 4 that the CNTs/C@Fe/CS could be well dispersed in water and can be easily separated by using a magnet.

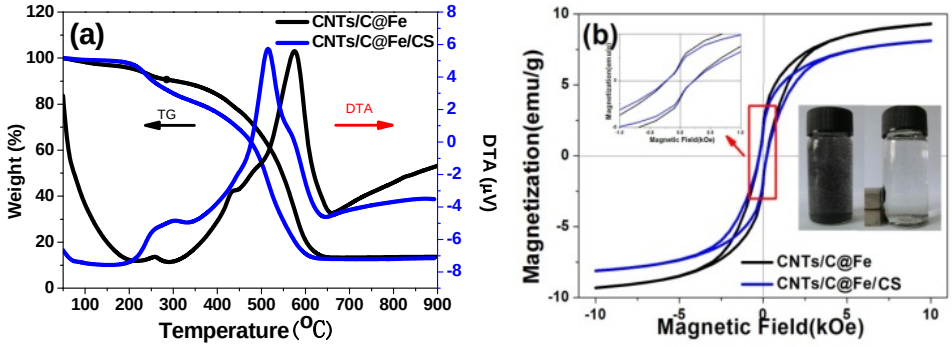

Fig. 4 Characterization of CNTs/C@Fe and CNTs/C@Fe/CS, (a) TGA, (b) magnetization characteristics.

3.3 Adsorption isotherms

Equilibrium adsorption isotherm is one of the most important data to elucidate the adsorption mechanism, and then four typical isotherm equations were selected to describe the adsorption process as shown in Fig. 5, the parameters are shown in Table 1. In Langmuir model, the q_{max} and K_L increases with increase in temperature due to the endothermic nature of the adsorption

Physical Chemistry Chemical Physics Accepted Manuscript

process. The R_L values were between 0 and 1, proving that the adsorption is a favorable process. Maximum adsorption capacities of tetracycline on different adsorbents based on Langmuir model are shown in Table 2. The high correlation coefficients for all temperatures indicate that the adsorption of tetracycline on CNTs/C@Fe/CS is in compliance with the Freundlich isotherm. The high values of K_F indicate a high adsorption capacity and good affinity between tetracycline and CNTs/C@Fe/CS. The 1/n values are far less than 1, implying that favorable adsorption at all temperatures studied. The increase of Freundlich constants (K_F) with increase of temperature suggests that high temperature favors adsorption and the adsorption is endothermic in nature. It is found that the plots of Tempkin are deviate from linearity at all the temperatures. In D-R model, the q_m was different from q_e derived from the Langmuir. The difference may be attributed to the different definition of maximum adsorption capacity in two models. In Langmuir model, q_e represents the maximum adsorption at monolayer coverage, whereas q_m represents the maximum adsorption at the total specific micropore volume of the adsorbent in D-R model. The mean adsorption energy (E) was found to be lower than the range of adsorption reaction 8–16 kJ/mol [31].

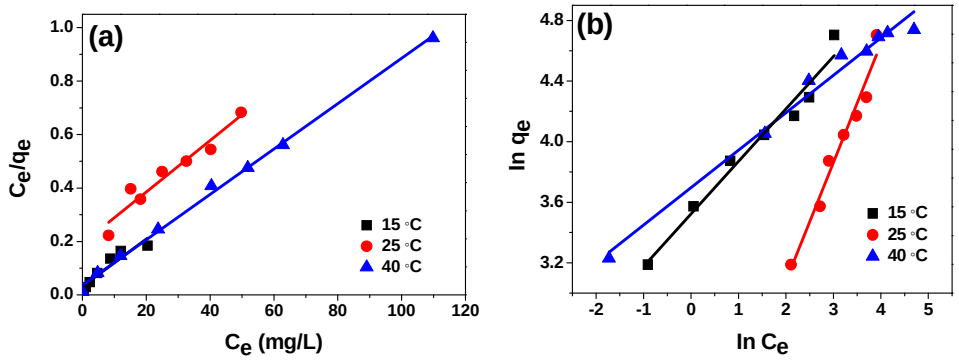

Physical Chemistry Chemical Physics Accepted Manuscript

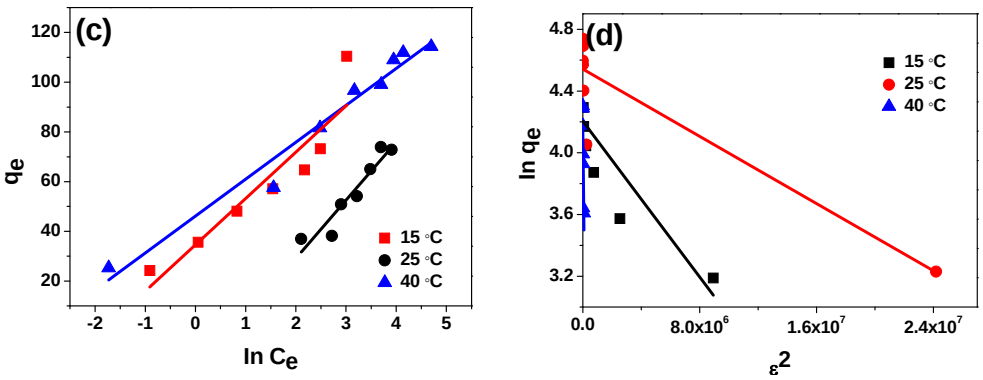

Fig. 5 Adsorption isotherms at different temperatures (15 ℃, 25 ℃ and 40 ℃, 100 mg/L, 1 mg/mL, 24 h). (a) Langmuir model, (b) Freundlich model, (c) Temkin model, (d) D-R model.

Table 1 The parameters derived from the Langmuir, Freundlich, Temkin, and D-R models.

Isotherm model	Parameters	15℃	25℃	40℃
Langmuir	q_m(mg/g)	103	104	117
	K_L($\times10^3$ L/mg)	0.05	0.21	0.35
	R_L	0.22	0.66	0.32
	R^2	0.82	0.95	0.94
Freundlich	K_F (L/g)	4.55	30.30	33.87
	n	2.88	1.28	4.04
	R^2	0.96	0.98	0.96
Temkin	K_T (L/mol)	2.49	4.29	22.09
	B_T	18.65	23.35	14.86
	R^2	66.69	0.84	0.89
D-R	q_m(mg/g)	79.84	93.69	64.07
	ß(mol^2/kJ^2)	1.26	0.54	0.08
	E(kJ/mol)	0.62	0.96	2.5
	R^2	0.76	0.85	0.83

Table 2 Maximum adsorption capacities of tetracycline on different adsorbents based on Langmuir model.

Physical Chemistry Chemical Physics Accepted Manuscript

Adsorbent	q_m (mg/g)	Reference
GO functionalized magnetic particles	39.1	[32]
Macroporous polystyrene resins	98.04	[33]
Modified bio-char	17.0	[34]
Activated carbon	475.48	[35]
CNTs/C@Fe/CS	104	This study

3.4 Adsorption Kinetics

In order to analyze the sorption kinetics, the pseudo-first-order the pseudo-second-order and the intra-particle diffusion model were applied to the experimental data as shown in Fig. 6. It is obvious from Table 2 that the correlation coefficients R^2 for the linear plots of the pseudo-second-order model is higher than the correlation coefficients R^2 for the pseudo-first-order. This indicates that the adsorption kinetic is better represented by the pseudo-second-order model. The intraparticle diffusion model was proposed to identify the adsorption mechanism and to predict the rate controlling step, where C is the intercept and kdiff. ($mg/g \cdot min^{0.5}$) is the intraparticle diffusion rate constant. The intraparticle diffusion model usually includes three steps. The first portion is the external surface adsorption or boundary layer diffusion. The second portion is the gradual stage of adsorption which is the intraparticle diffusion. If the plot of q_t versus $t^{0.5}$ is linear and passes through the origin, then the intraparticle diffusion is the rate-controlling step. In this adsorption, though the q_t and $t^{0.5}$ had linear relationship, the plot did not pass through the origin, so the process is not rate-controlling [36].

Physical Chemistry Chemical Physics Accepted Manuscript

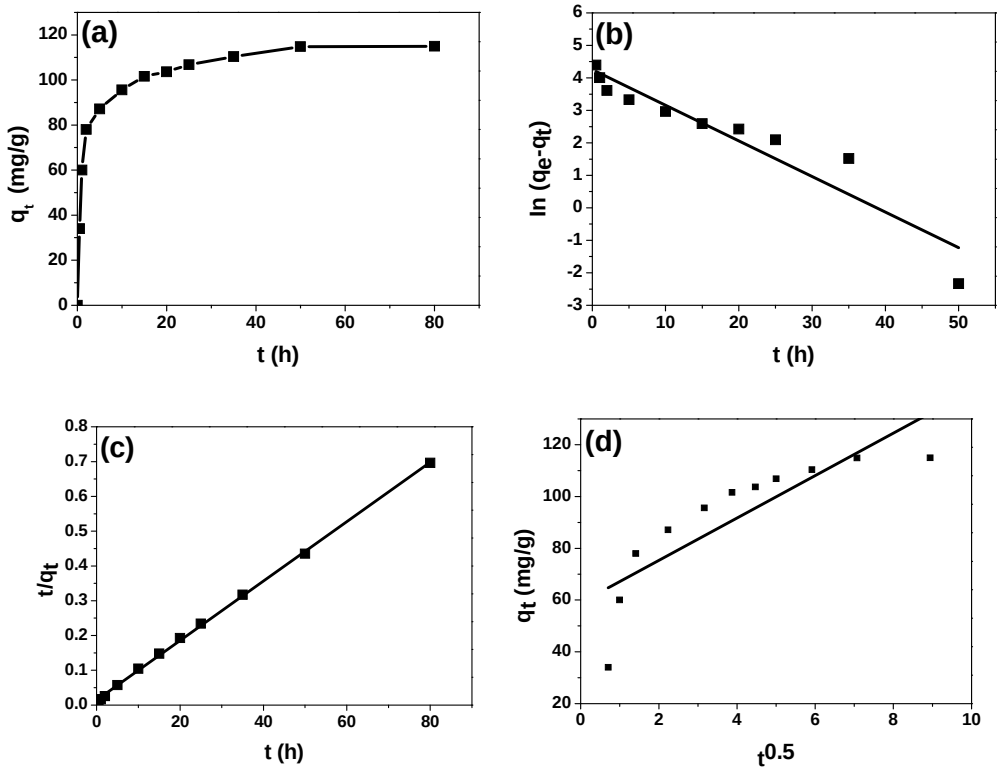

Fig. 6 Kinetic curves (a), kinetics analyses of pseudo-first order model (b), pseudo-second order model (c), and intra-particle diffusion model (d). (25 ℃, 100 mg/L, 1 mg/mL).

Table 2 Kinetic parameters of pseudo first- and second-order adsorption kinetic models and intra-particle diffusion model.

pseudo-first order			pseudo-second order			Intra-particle diffusion		
q_e(mg/g)	k_1(min^{-1})	R^2	q_e(mg/g)	k_2(min^{-1})	R^2	k_{id}(mg/g•min$^{0.5}$)	C(mg/g)	R^2
69.4	0.004	0.88	117.6	0.004	0.99	8.2	58.9	0.97

3.5 Influence of pH

Influence of pH on adsorption is shown in Fig. 7a. Tetracycline is an amphoteric molecule with multiple ionizable functional groups: a tricarbonylamide group, a phenolic diketone group, and a dimethyl amino group. Tetracycline can undergo protonation-deprotonation reactions and present different species depending on the solution pH. Dissolved tetracycline species may have net charges that are positive (H_3TC^+, pH < 3.3), neutral

Physical Chemistry Chemical Physics Accepted Manuscript

(H_2TC^0, 3.3< pH< 7.68), one negative (HTC^-, 7.68 < pH< 9.68) or two negative (TC^{2-}, pH > 9.68) [37]. It can be seen from Fig. 5b that the adsorption of tetracycline was pH-dependent. CNTs/C@Fe/CS had larger adsorption capacity under alkaline solution than acid circumstances. This result might be attributed to the molecular structure of tetracycline and the functional groups present on the surface of the CNTs/C@Fe/CS. Possibly, the deprotonation of carboxyl groups of the CNTs/C@Fe/CS was enhanced under alkaline conditions, which strengthened the electrostatic interaction with amino groups on tetracycline [38]. Moreover, the variation in pH not only focuses on the protonation–deprotonating transition of functional groups, but also results in a change in chemical speciation [39]. Therefore, cation exchange reactions, as well as surface complexation are expected to occur between the zwitterionic tetracycline molecules and the respective ionic/polar sites on the adsorbent surface. Moreover, the strong interactions of tetracycline directly with the surface of carbon nanotube cannot be ignored[40].

To evaluate the effects of heavy metals and organic matters on the adsorption, Cu^{2+} or humic acid was simultaneously adsorbed with tetracycline respectively as shown in Fig. 7b. The adsorption of tetracycline on CNTs/C@Fe/CS is enhanced with an increase in Cu^{2+} concentration. It was because that tetracycline has multiple ionizable functional groups and various species in solution, which exhibit strong complexing capability with Cu^{2+}, tetracycline and Cu^{2+} might facilitate the sorption of each other by the formation of tetracycline–Cu^{2+} complexes with higher sorption affinity, and/or by the formation of surface-bridging mechanism [41]. Humic acid could also promote the adsorption of tetracycline on CNTs/C@Fe/CS. It was because that tetracycline could be adsorbed by humic acid consistent with complexation between the cationic/zwitterionic tetracycline species and deprotonated functional groups in humic acid. Therefore, in the CNTs/C@Fe/CS–humic acid–tetracycline ternary system, tetracycline can either complex with the surface sites of CNTs/C@Fe/CS or interact with dissolved humic acid in solution or humic acid sorbed with CNTs/C@Fe/CS surfaces. It is reasonable to

Physical Chemistry Chemical Physics Accepted Manuscript

speculate that humic acid might act as a bridge to complex with both CNTs/C@Fe/CS surfaces and tetracycline molecules [42].

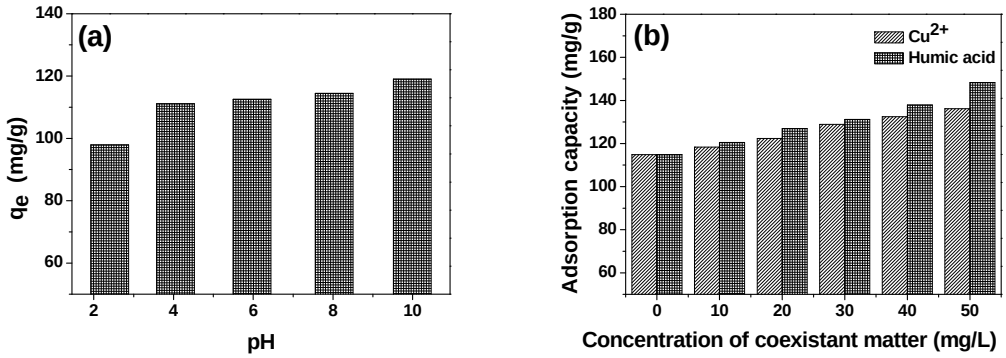

Fig. 7 Influence of pH(a), Cu^{2+} and humic acid (b) on tetracycline adsorption on CNTs/C@Fe/CS.

3.6 Characterization of CNTs/C@Fe/CS before and after adsorption

FTIR of CNTs/C@Fe/CS before and after adsorption are shown in Fig.8a, it can be seen that CNTs/C@Fe/CS contains many functional groups. Band at 1089 cm^{-1} is assigned to the C–O bonds and band at 1227 cm^{-1} which is assigned to the C–OH [43]. Amide I (due to the high C=O group extinction coefficient) and NH_2 bands at 1647 cm^{-1} and 1590 cm^{-1}; the band at around 3400 cm^{-1} is assigned to O-H, as well as to intermolecular hydrogen bonding [44]. After adsorption, these bonds became weaker indicating chemical adsorption existed. XPS of CNTs/C@Fe/CS before and after adsorption are shown in Fig.8b. It can be seen that CNTs/C@Fe/CS does not have N1s peak before adsorption, however, the N1s appears in CNTs/C@Fe/CS after adsorption as the tetracycline contains abundant N elements. N_2 adsorption and desorption curves of CNTs/C@Fe/CS before and after adsorption are shown in Fig. 8c and the pore size distributions are shown in Fig. 8d. The specific area of CNTs/C@Fe/CS reduced after adsorption, indicating physical adsorption took place. The total pore volume reduced further proved that after adsorption the tetracycline occupied pores of CNTs/C@Fe/CS. Fig. 9 shows the loss of adsorption capacity of adsorbent which was reused 10 times after regeneration. The adsorption capacity still maintained 99.3 mg/g after 10 times, which demonstrated an extended useful lifetime for the adsorbent. Hence, it can

Physical Chemistry Chemical Physics Accepted Manuscript

be seen that the CNTs/C@Fe/CS has significant potential to be used as an adsorbent.

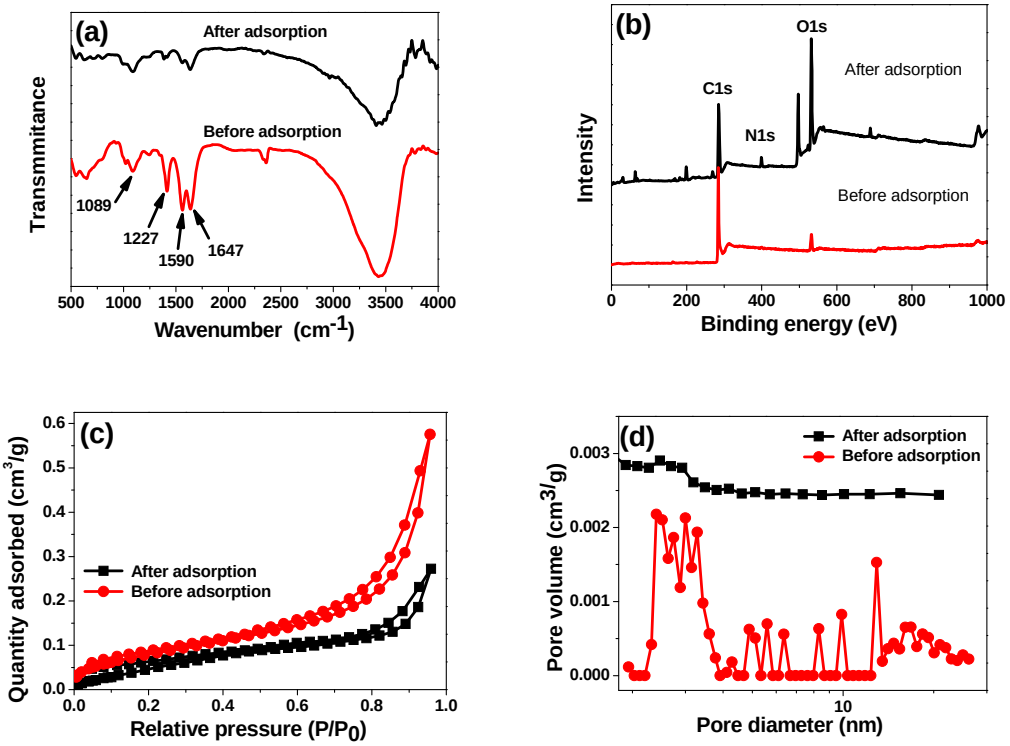

Fig. 8 FTIR (a), XPS (b), N_2 adsorption and desorption curves (c), and pore size distributions (d) characterization of CNTs/C@Fe/CS before and after adsorption.

Table 3 Specific surface area and pore values of CNTs/C@Fe/CS before and after adsorption.

Sample	Before adsorption	After adsorption
Specific surface area (m^2/g)	6.8	5.1
Average pore size (nm)	7.8	10.6
Total pore volume (m^3/g)	0.0196	0.0093

Physical Chemistry Chemical Physics Accepted Manuscript

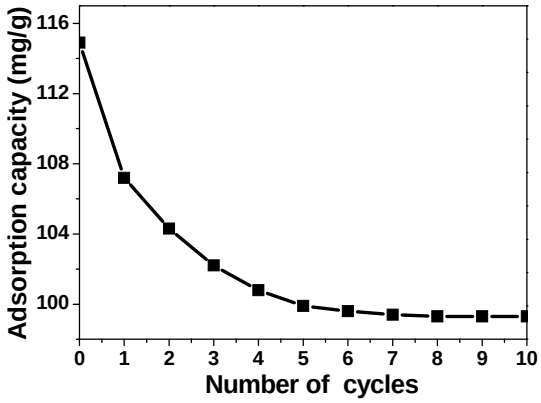

Fig. 9 Regeneration properties of adsorbent.

4. Conclusions

A new kind of magnetic biocomposite(CNTs/C@Fe/CS) prepared based on the as-prepared carbon nanotubes(APCNTs), metal nanoparticles in APCNTs can be utilized directly without any purification treatment, and the carbon shells provide an effective barrier against oxidation, acid dissolution, and movement of MNPs, and thus ensure a long-term stability of CNTs/C@Fe/CS. The addition of CS brought more oxygen containing functional groups and be beneficial to the enhanced adsorption capacity (104 mg/g) for the removal of tetracycline from aqueous solutions. The composite had good magnetization characteristics, even in acid solutions, and the CNTs/C@Fe/CS adsorbents could be effectively and quickly separated by applying an external magnetic field. Therefore, CNTs/C@Fe/CS is a promising magnetic nanomaterial for the removal of organic pollutants for environmental remediation.

Acknowledgements

This research was supported by the National Natural Science Foundation of China (No. 21207100, 51408362)

References

Physical Chemistry Chemical Physics Accepted Manuscript

1. Y. Zhuang, F. Yu, J. Ma and J. H. Chen, *New Journal of Chemistry*, 2015.

2. C. Song, X.-F. Sun, S.-F. Xing, P.-F. Xia, Y.-J. Shi and S.-G. Wang, *Environmental Science and Pollution Research*, 2013, **21**, 1786-1795.

3. J. G. da Silva, M. A. Hyppolito, J. A. de Oliveira, A. P. Corrado, I. Y. Ito and I. Carvalho, *Bioorg. Med. Chem.*, 2007, **15**, 3624-3634.

4. M. Peterson, *J. Feline Med. Surg.*, 2012, **14**, 804-818.

5. J. L. Acero, F. J. Benitez, A. I. Leal, F. J. Real and F. Teva, *Journal of hazardous materials*, 2010, **177**, 390-398.

6. F. Yu, J. Ma and D. Bi, *Environmental Science and Pollution Research*, 2014, 1-10.

7. F. Yu, J. Ma and S. Han, *Sci Rep-Uk*, 2014, **4**.

8. W. T. Audenaert, D. Vandierendonck, S. W. Van Hulle and I. Nopens, *Water research*, 2013, **47**, 2387-2398.

9. A. Justo, O. Gonzalez, J. Acena, S. Perez, D. Barcelo, C. Sans and S. Esplugas, *Journal of hazardous materials*, 2013, **263 Pt 2**, 268-274.

10. I. Chopra and M. Roberts, *Microbiology and molecular biology reviews : MMBR*, 2001, **65**, 232-260 ; second page, table of contents.

11. L. Ji, W. Chen, L. Duan and D. Zhu, *Environmental science & technology*, 2009, **43**, 2322-2327.

12. F. Yu, J. H. Chen, M. X. Yang, L. Zhou, L. Jin, C. Su, F. L. Li, L. Chen, Z. W. Yuan, L. L. Yu and J. Ma, *New Journal of Chemistry*, 2012, **36**, 1940-1943.

13. J. Ma, F. Yu, L. Zhou, L. Jin, M. X. Yang, J. S. Luan, Y. H. Tang, H. B. Fan, Z. W. Yuan and J. H. Chen, *Acs Appl Mater Inter*, 2012, **4**, 5749-5760.

14. F. Yu, J. H. Chen, L. Chen, J. Huai, W. Y. Gong, Z. W. Yuan, J. H. Wang and J. Ma, *J Colloid Interf Sci*, 2012, **378**, 175-183.

15. V. K. Gupta, S. Agarwal and T. A. Saleh, *Water research*, 2011, **45**, 2207-2212.

16. J. Ma, F. Yu, Z. Wen, M. Yang, H. Zhou, C. Li, L. Jin, L. Zhou, L. Chen, Z. Yuan and J. Chen, *Dalton transactions*, 2013, **42**, 1356-1359.

17. C. Lau, M. J. Cooney and P. Atanassov, *Langmuir*, 2008, **24**, 7004-7010

18. L. Carson, C. Kelly-Brown, M. Stewart, A. Oki, G. Regisford, Z. Luo and V. I. Bakhmutov, *Mater Lett*, 2009, **63**, 617-620.

19. L. Qian and X. Yang, *Talanta*, 2006, **68**, 721-727.

Physical Chemistry Chemical Physics Accepted Manuscript

20. L. Chen, J. Hu, X. Shen and H. Tong, *Journal of materials science. Materials in medicine*, 2013, **24**, 1843-1851.

21. J. Ma, Z. Zhu, B. Chen, M. Yang, H. Zhou, C. Li, F. Yu and J. Chen, *Journal of Materials Chemistry A*, 2013, **1**, 4662.

22. J. Venkatesan, R. Jayakumar, A. Mohandas, I. Bhatnagar and S.-K. Kim, *Materials*, 2014, **7**, 3946-3955.

23. Y. Zhuang, X. Wu, Z. Cao, X. Zhao, M. Zhou and P. Gao, *Materials science & engineering. C, Materials for biological applications*, 2013, **33**, 4732-4738.

24. B. S. Tawabini, S. F. Al-Khaldi, M. M. Khaled and M. A. Atieh, *J Environ Sci Heal A*, 2011, **46**, 215-223.

25. S. A. Ntim and S. Mitra, *Abstr Pap Am Chem S*, 2010, **240**.

26. S. A. Ntim and S. Mitra, *J. Colloid Interface Sci.*, 2012, **375**, 154-159.

27. S. A. Ntim and S. Mitra, *J Chem Eng Data*, 2011, **56**, 2077-2083.

28. J. Ma, J. N. Wang and X. X. Wang, *Journal of Materials Chemistry*, 2009, **19**, 3033-3041.

29. X. Wang, R. Sun and C. Wang, *Colloids Surf. Physicochem. Eng. Aspects* 2014, **441**, 51-58.

30. G. Zhao, J. Li and X. Wang, *Chemical Engineering Journal*, 2011, **173**, 185-190.

31. W. Wang, B. Zheng, Z. Deng, Z. Feng and L. Fu, *Chemical Engineering Journal*, 2013, **214**, 343-354.

32. Y. Lin, S. Xu and J. Li, *Chemical Engineering Journal*, 2013, **225**, 679-685.

33. Y. Chao, W. Zhu, B. Yan, Y. Lin, S. Xun, H. Ji, X. Wu and H. Li, Changri, *Journal of Applied Polymer Science*, 2014 **131**, 40561.

34. P. Liu, W. J. Liu, H. Jiang, J. J. Chen, W. W. Li and H. Q. Yu, *Bioresource technology*, 2012, **121**, 235-240.

35. L. Huang, M. Wang, C. Shi, J. Huang and B. Zhang, *Desalination and Water Treatment*, 2014, **52**, 2678-2687.

36. D. K. Mahmoud, M. A. M. Salleh, W. A. W. A. Karim, A. Idris and Z. Z. Abidin, *Chemical Engineering Journal*, 2012, **181-182**, 449-457.

37. Y. Zhao, F. Tong, X. Gu, C. Gu, X. Wang and Y. Zhang, *Sci. Total. Environ.*, 2014, **470-471**, 19-25.

Physical Chemistry Chemical Physics Accepted Manuscript

38. L. Zhao, P. Dong, J. Xie, J. Li, L. Wu, S.-T. Yang and J. Luo, *Mater. Res. Express.*, 2013, **1**, 015601.

39. E. E. Ghadim, F. Manouchehri, G. Soleimani, H. Hosseini, S. Kimiagar and S. Nafisi, *PLOS ONE* 2013, **8**, e79254.

40. L. Obeid, N. El Kolli, N. Dali, D. Talbot, S. Abramson, M. Welschbillig, V. Cabuil and A. Bee, *Journal of colloid and interface science*, 2014, **432**, 182-189.

41. F. Lian, Z. Song, Z. Liu, L. Zhu and B. Xing, *Environmental pollution*, 2013, **178**, 264-270.

42. Y. Zhao, J. Geng, X. Wang, X. Gu and S. Gao, *Journal of colloid and interface science*, 2011, **361**, 247-251.

43. Z. Yuan, Y. Fei, M. Jie and C. Junhong, *RSC Advances*, 2015, **5**, 27964-27969.

44. A. L. Caroni, C. R. de Lima, M. R. Pereira and J. L. Fonseca, *Colloids and Surfaces B: Biointerfaces*, 2012, **100**, 222-228.

Physical Chemistry Chemical Physics Accepted Manuscript